

Electrodynamics in light of the new paradigm: New insights

Yefim Bakman, bakmanyef@gmail.com

Tel Aviv, April 29, 2024

Abstract. Standard physics education provides no opportunities to realize that electrical interactions are based on gravitational forces because gravity never shows repulsion. Even when the universe exhibits repulsion in the form of "dark energy," physicists do not recognize that this phenomenon arises from gravity.

The new paradigm described herein breaks through this stereotype. According to the new paradigm, gravity not only underlies the phenomenon of dark energy, but is also the basis of electrical interactions. This new understanding of electric charge and magnetism allows us to find simple explanations for many phenomena in this domain. The new paradigm also demonstrates the inconsistency of Faraday's law of induction in the performed experiment.

1. Introduction

The conventional understanding of gravity includes a mistake: it is traditionally believed that only massive bodies can create gravity. It remained difficult to argue with this statement until the phenomena of dark matter and energy were discovered.

As the problem of dark energy remains unresolved, many physicists have concluded that the underlying hypotheses are incorrect; thus, a deep revision of the physical paradigm has become urgent, as cosmetic corrections are not effective.

In 2020, a new paradigm [1] was published that provides a breakthrough in understanding gravity [2]. According to this paradigm, a gravitational field can exist in the absence of massive bodies, and the phenomena of dark matter and dark energy are variants of this extended concept of gravity.

The unification arising from this new paradigm extends to electrodynamics. According to the new paradigm, an electric field is a manifestation of the dynamic gravitational field created by electrons and other charges.

Here, we demonstrate how the new paradigm provides a correct view of the fundamentals of electrodynamics and reduces the number of contradictions in this field.

2. How gravity works

According to the new paradigm [1], there exists an invisible unorganized mass, from which, under certain conditions, ordinary mass arises. This unorganized mass is present everywhere as the background of all phenomena. Following Tesla [3] and starting from previous work [4], the unorganized mass is called the "primary substance," indicating the primary material from which the universe was created.

The primary substance is not only the universal building material for mass creation but is also the universal medium. A gravitational field is a zone of primary substance with inhomogeneous density (Fig. 1) [2]. This understanding reveals the true cause of gravity [5].

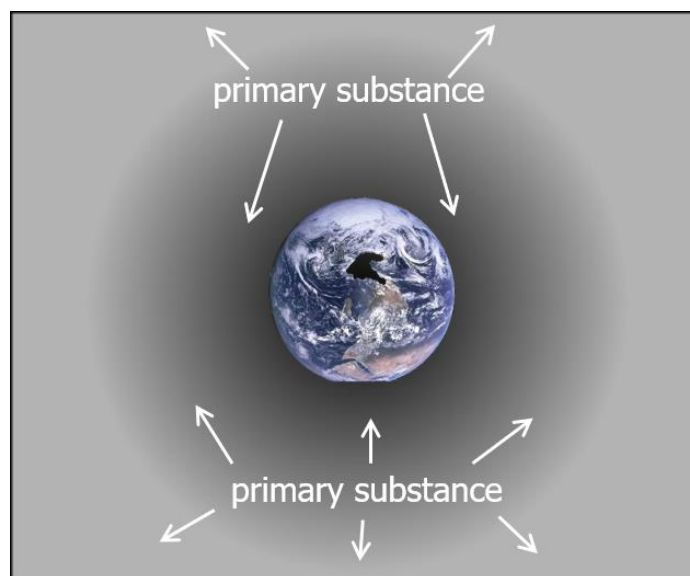


Fig. 1. An image of Earth, surrounded by the primary substance. Although the primary substance is invisible, it is depicted in shades of gray in this figure; darker shading corresponds to a higher density of the primary substance.

According to the new paradigm, elementary particles, atoms, and molecules are stable vortices of the primary substance (Fig. 2).

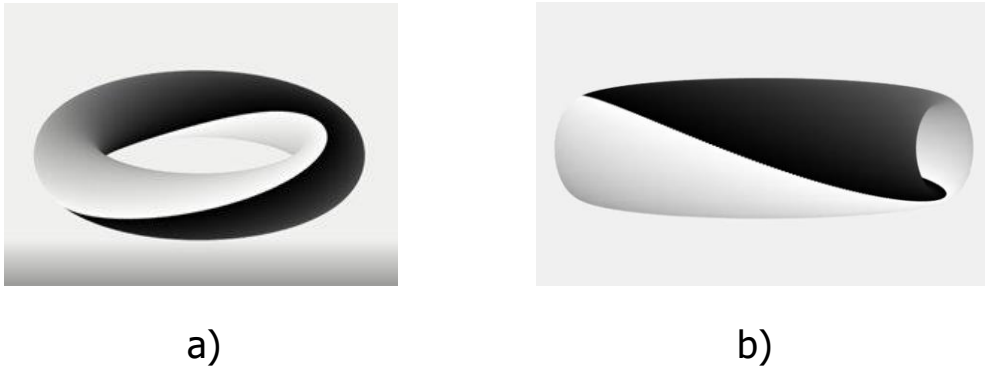


Fig. 2. An electron vortex (a) and a photon vortex (b). The photon has a toroidal shape similar to that of an electron, but highly elongated.

The electron density wave participates in two rotations. One rotation around the toroid creates the spin of an electron. The second rotation in the cross-section of the toroid creates an electrical charge.

The vortex model of elementary particles allows us to reveal the mechanism of free-fall acceleration in a gravitational field. For clarity, we use a flat illustration of a vortex in Fig. 3.

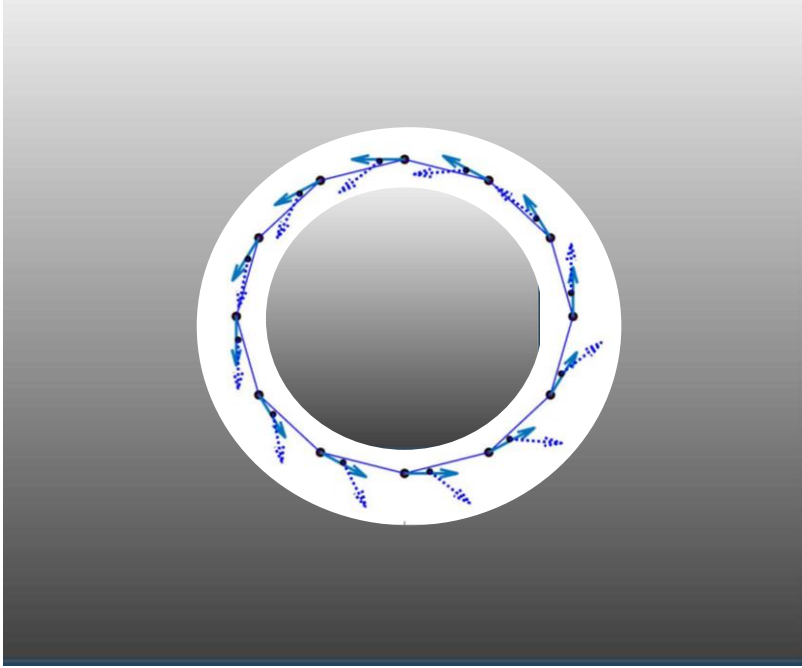


Fig. 3. Flat illustration of the speed deviations of a vortex wave in a gravitational field. The medium density is higher in the lower part of the figure. The particle is motionless. After a time interval dt , the velocities of points on the wave front deviate. The new directions of the velocities are shown by dotted lines.

The velocity deviation shown in Fig. 3 was calculated in [6]: in a region of primary substance with inhomogeneous density, the velocity v of each point on the vortex wave front deviates over the time interval dt by an angle:

$$d\alpha = \nabla u \sin \alpha dt \quad (1)$$

where u is the density wave velocity and α is the angle between ∇u and the direction of \vec{u} . Here, ∇u is an indicator of the gravitational strength. The vertical acceleration a_z of a point on the wave front is as follows:

$$a_z = -v \nabla u \sin^2 \alpha \quad (2)$$

As can be seen from Eq. (2), the vertical component of the acceleration of a point is always negative, i.e., the wave speed deviates downward, toward a higher density of the medium.

The free-fall acceleration of a vortex occurs without any force, due to the energy of the inhomogeneous primary substance.

This phenomenon has some similarity with wind, which is caused by a heterogeneity of atmospheric pressure. If the atmospheric pressure is homogeneous, there is no wind. Similarly, there is no gravity in homogeneous primary substance.

The phenomenon of dark energy occurs in a region of space with a lower density of primary substance (Fig. 4). Because gravitational acceleration is always directed toward higher density, stars and galaxies accelerate outward.

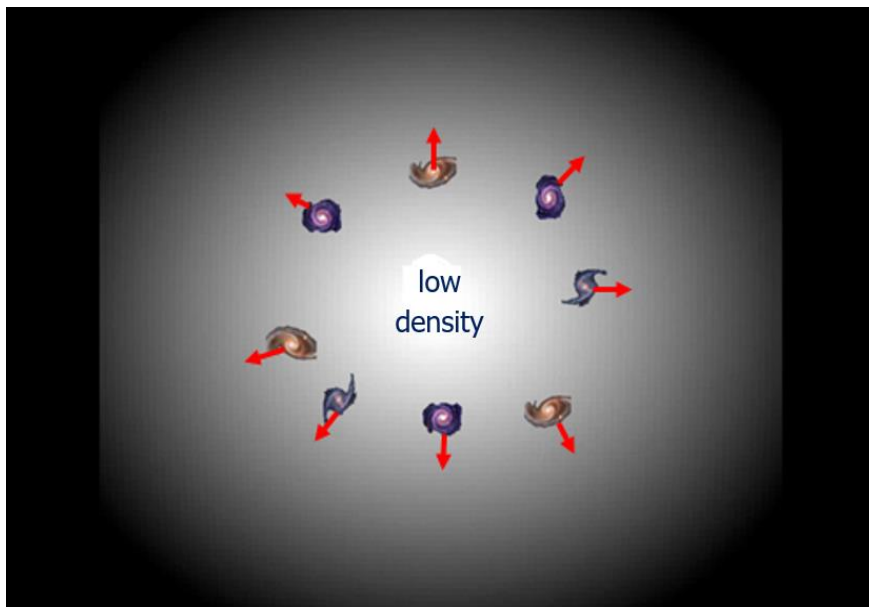


Fig. 4. A zone with a lower density of primary substance results in an inverse gravitational field, where stars and galaxies are accelerated outward.

3. Electric charge of an electron in the new paradigm

An electron vortex was shown in Fig. 3, whereas Fig. 5 schematically displays an electron as a cross-section.

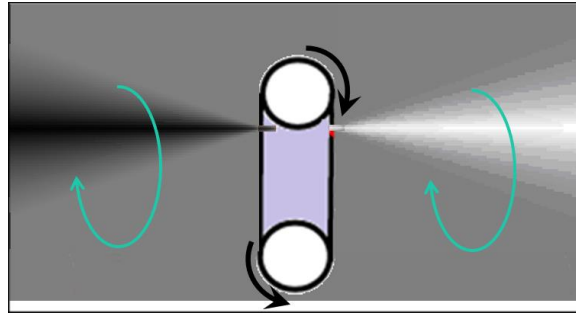


Fig. 5. Illustration of the charge of an electron. The gray shading shows the change in medium density caused by the behavior of the electron vortex [7].

On one side of the electron, a region of reduced medium density is formed, and on the opposite side, a region of increased medium density is formed. Thus, the electron's charge is a gravitational dipole, which is constantly created by the electron vortex circulation.

In Fig. 5, the gray shading indicates different densities of the primary substance: low density in white (negative charge), high density in black (positive charge), and intermediate density in gray.

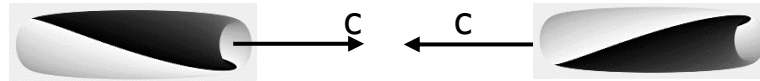
In contrast to an electric field, an ordinary gravitational field can be created by the complete disintegration of particles and atoms, which rarely occurs under normal conditions. Hence, gravitational interactions are weak compared with electrical interactions.

To clarify this difference further, imagine a fan moving air from one side to the other. This situation is similar to an electron and its charge.

Instead of a fan, we can consider a chemical reaction that creates a mixture of nitrogen and oxygen from chemicals. This case corresponds to ordinary gravity: it consumes materials and requires technological complications. In contrast, the fan does not consume materials and is technologically simple. An electric charge is created in a similar way.

The creation of a positron has been described in [7], as illustrated in Fig. 6.

Stage I. Two photons collide.



Stage II. Two photons stick together and shrink. Electric charges appear.



Stage III. The formed electron and positron separate and travel in different directions in a perpendicular magnetic field.

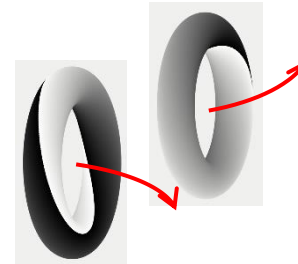


Fig. 6. Stages of collision of two photons. At suitable photon energies, one photon transforms into an ordinary electron with a negative charge in front of it, and the other photon transforms into a positron with a positive charge in front. Here, the magnetic field is perpendicular to the illustration.

We can also consider the situation shown in Fig. 7. In this figure, electron B is located between electrons A and C. To the left of electron B, the medium density is reduced by electron A, and to the right, the density is increased by electron C. Because of this density difference, electron B experiences gravitational acceleration to the right.

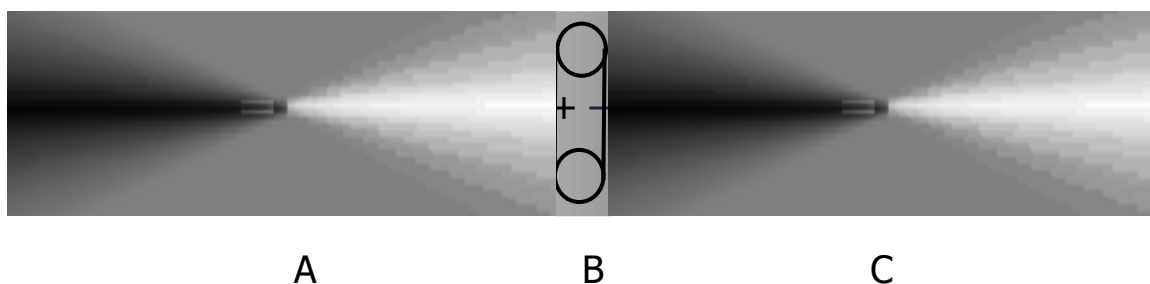


Fig. 7. The inhomogeneous density of the medium created by the charges of electrons A and C (electrons A and C themselves are not shown). The force on electron B has the same origin as the gravitational force.

Let us consider a chain of such electrons. For each electron B, the electron to the left faces electron B with a negative charge and hence pushes B to the right. At the same time, the electron to the right of electron B faces B with a positive charge and therefore pulls B toward the right.

If a sequence of free electrons oriented in this way closes into a ring, a microcurrent is obtained (Fig. 8).

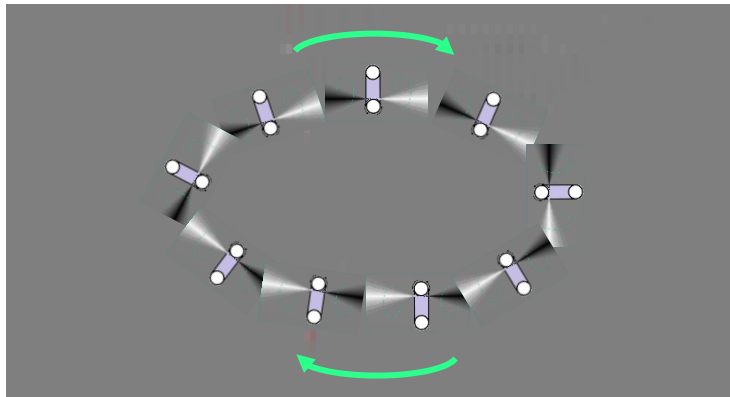


Fig. 8. Illustration of a microcurrent: Free electrons form a rotating chain.

Thus, the first requirement for a material to be magnetic is that it must contain free electrons. Second, magnetic microcurrents must be equally oriented (Fig. 9 left) and must retain this order. This state is usually called a magnetized state.

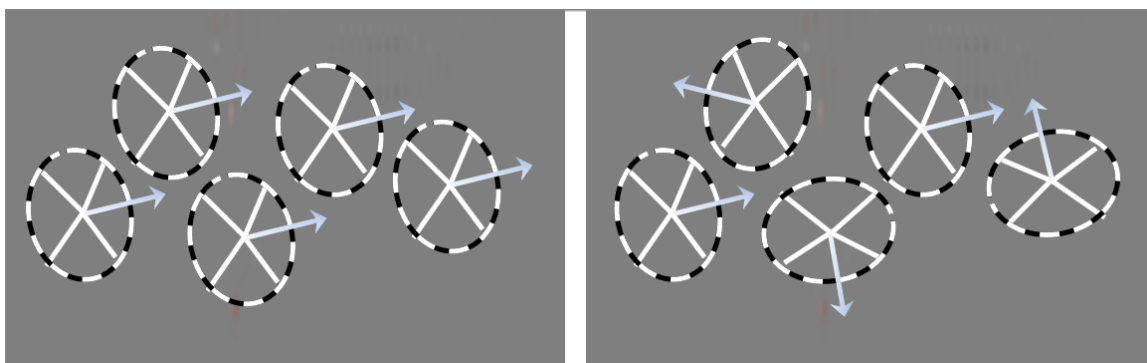


Fig. 9. Ampere's microcurrents shown schematically as dotted ovals in a magnetized (left) and demagnetized (right) state.

In non-magnetic metals, free electrons can link into chains (Fig. 10). When a current source is used, the chains move forward and form a macrocurrent.

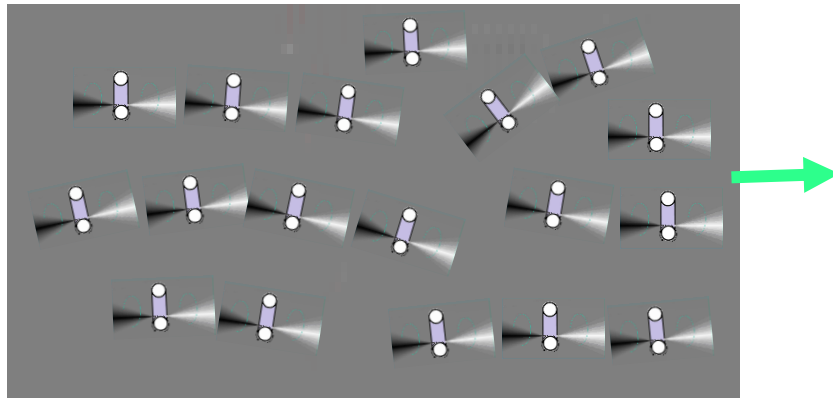


Fig. 10. Illustration of a macrocurrent: Under the influence of an EMF source, free electrons are oriented in one direction and form chains.

The ends of a coil with current play the role of magnetic poles: opposite poles attract (Fig. 11 top), and like poles repel (Fig. 11 bottom). Thus, a coil with current imitates a magnet. Because the turns of the coil are wound in the same direction, they provide a replacement for magnetization.

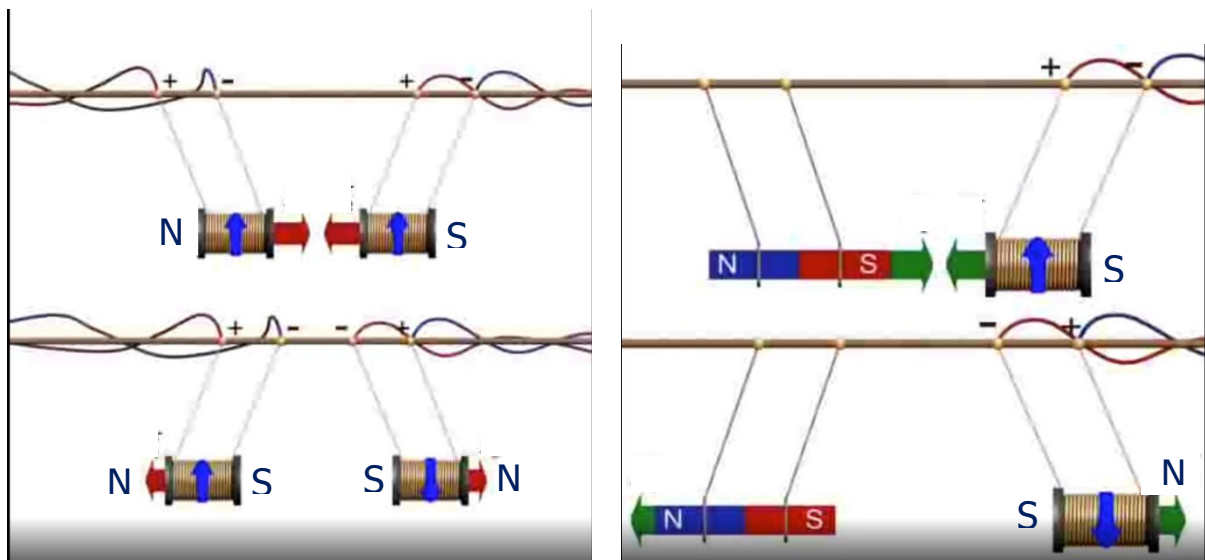


Fig. 11. Coils and magnets are interchangeable.

4. Ampère's and Weber's formulas

When Ampère published his famous work 200 years ago, there were difficulties in using his formula:

$$dF = -\frac{\mu_0 I I' ds ds'}{4\pi r^2} (2 \cos \varepsilon + 3 \cos \theta \cos \theta') \quad (3)$$

where ε is the angle between infinitesimal vectors ds and ds' , r is the distance between these vectors, and $\pi - \theta'$ is the angle between ds' and \vec{r} .

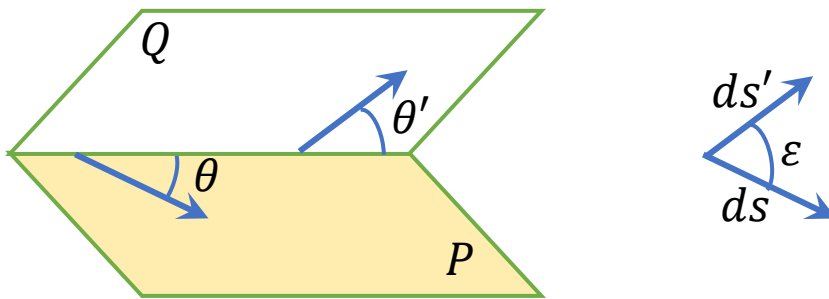


Fig. 12. Angles between current elements ds , ds' , and \mathbf{r} .

Only the simplest cases were integrable, such as the attraction/repulsion of parallel wires carrying current.

Since then, a more convenient vector form has been found (Eq. (4)); instead of three angles, the dot product is used, which, for the case of orthogonal coordinates, does not require the cosines of angles [8]:

$$\mathbf{F}_{12} = -\frac{\mu_0 I_1 I_2}{4\pi} \mathbf{r} \left[\frac{2(ds_1 \cdot ds_2)}{r^3} - \frac{3(\mathbf{r} \cdot ds_1)(\mathbf{r} \cdot ds_2)}{r^5} \right] \quad (4)$$

Ampère hypothesized that magnetism arises from microscopic electrical currents, with currents being more fundamental than magnets.

The new paradigm makes it possible to simulate magnets using microcurrents, expanding the scope of application of Ampère's formula.

Weber published his fundamental force law for moving charges in 1846 [9] [10]. His approach modifies the Coulomb electrostatic force to

account for the relative velocities of electrical particles without a magnetic field.

Assis [8] also found a convenient vector form for writing Weber's formula:

$$EMF = -\frac{\mu_0}{4\pi} \oint \oint \frac{(\mathbf{r} \cdot d\mathbf{s}_2)}{r^3} \left[2 I_1 (\mathbf{V} \cdot d\mathbf{s}_1) - 3 I_1 \frac{(\mathbf{r} \cdot \mathbf{V})(\mathbf{r} \cdot d\mathbf{s}_1)}{r^2} + \frac{\partial I_1}{\partial t} (\mathbf{r} \cdot d\mathbf{s}_1) \right] \quad (5)$$

From Weber's force formula, Maxwell derived Ampere's empirical law, and Assis [8] derived two cases of an induced electromotive force. These two cases are given in the next section.

5. Experimental testing

Electromagnetic induction requires two separate circuits; the primary circuit can be a magnet. An EMF occurs in the secondary circuit when at least one of the following conditions is met:

- a) there is movement of the primary circuit (now also a magnet) relative to the secondary circuit (e.g. the rotor and stator in a generator) or
- b) the current in the primary circuit changes (e.g. in transformers).

To experimentally test Weber's formula and the conclusions of the new paradigm, the first method was chosen. The experimental setup is shown in Fig. 13.

In this setup, the coil diameter is 40 mm, the magnet diameter is 15 mm, and g is the free-fall acceleration.

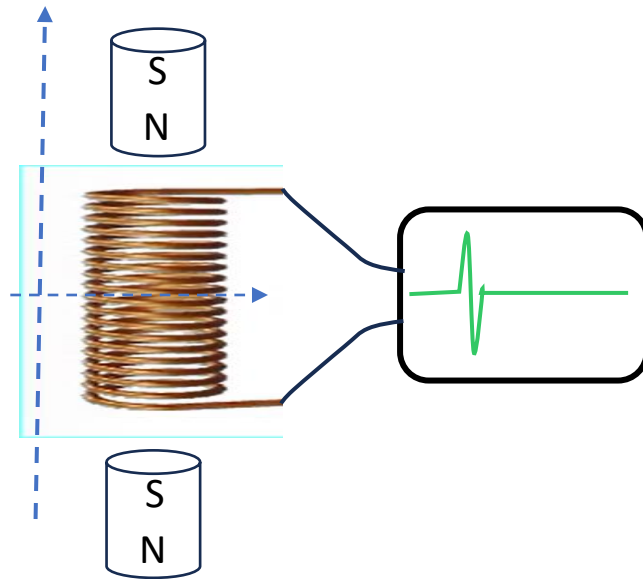


Fig. 13. Experimental setup.

We release a cylindrical magnet into the coil, and the magnet falls with a constant acceleration of gravity. In the process, we measure the voltage V on the coil.

The magnet's speed is $v = gt$, and its distance from the center of the coil is $r = \left| h - \frac{gt^2}{2} \right|$. Fig. 14 shows a screenshot of an oscilloscope (OSC482) while the cylindrical magnet falls through the coil.

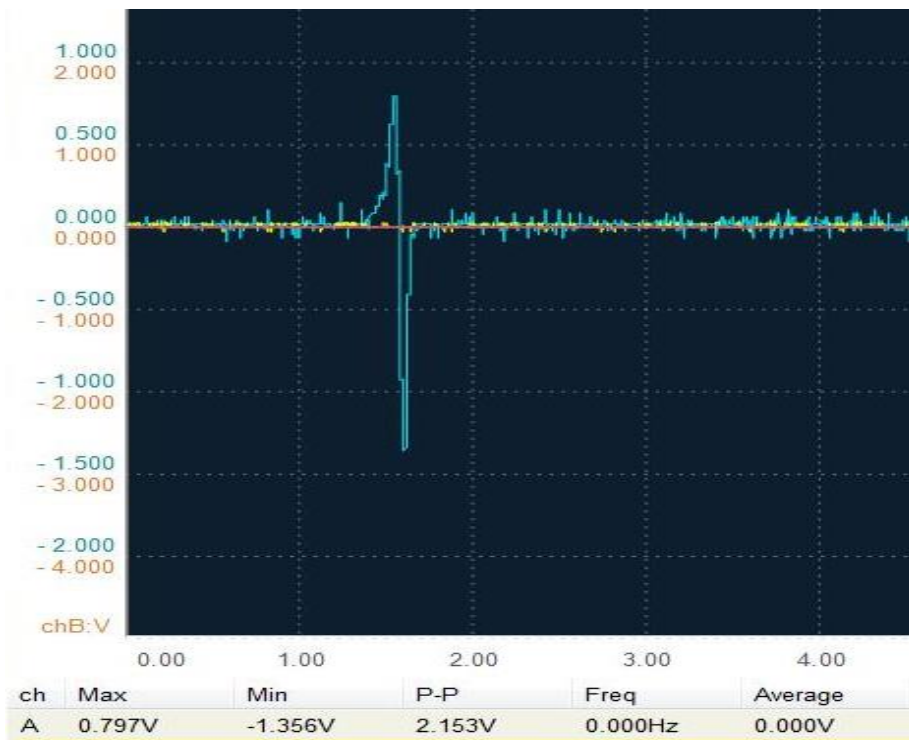


Fig. 14. Voltage $U(t)$ across a coil as a magnet falls through it. Screenshot 4 from Channel A (in blue) of the oscilloscope.

6. Simulation of a cylindrical magnet falling through a coil

Within the framework of classical electrodynamics, this experiment cannot be simulated. However, with the new paradigm, one can employ the microcurrent model and Weber's formula (Eq. (5)) to simulate this experiment.

For the calculation, a simple model is proposed in which the circular current falls with acceleration through the coil turn (Fig. 15). The force creating the emf on ds_2 is calculated by integrating over $d\alpha$ and dividing by ds_2 , which yields the force per unit length of the turn.

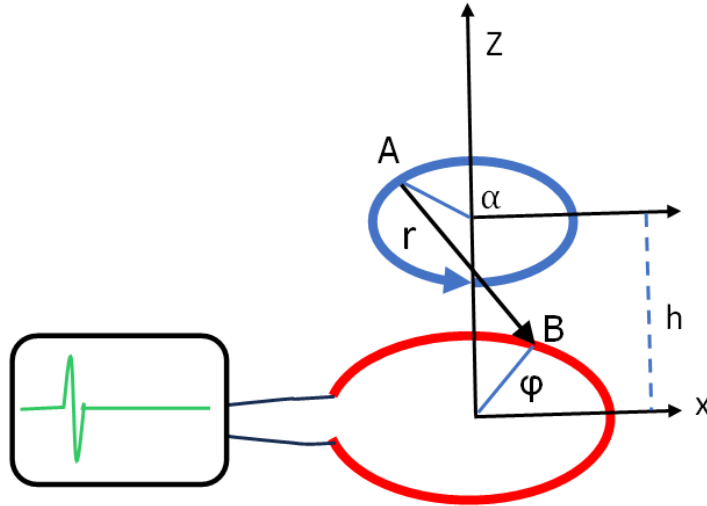


Fig. 15. Microcurrent model for the simulating the coil experiment.

We used an ad hoc version of Weber's formula (Eq. (6)). In this case, the term with the derivative of the current I_1 is removed from the formula, as the microcurrent of the magnet does not change.

Additionally, the dot product $\mathbf{V} \cdot d\mathbf{s}_1 = 0$, because the velocity vector \mathbf{V} is perpendicular to the x-y plane.

$$EMF(t) = \frac{\mu_0 I_1}{4\pi} \oint \frac{(\mathbf{r} \cdot d\mathbf{s}_2)}{r^3 |d\mathbf{s}_2|} \left[3 \frac{(\mathbf{r} \cdot \mathbf{V})(\mathbf{r} \cdot d\mathbf{s}_1)}{r^2} \right] \quad (6)$$

According to Feynman [11] (p. 17-1), the EMF is "the tangential component of the force on the charges throughout the length of the loop." The force on ds_2 is directed along \mathbf{r} ; thus, multiplying by $\frac{(\mathbf{r} \cdot d\mathbf{s}_2)}{r |d\mathbf{s}_2|}$ yields the tangential component of the EMF along the wire.

For the simulation, the element ds_2 was fixed at $\varphi=0$.

To obtain the total EMF, it is sufficient to multiply the result by the length of the coil wire, as all ds_2 elements are equivalent because of their axial symmetry.

As a result, numerical integration of the EMF over $d\alpha$ gives the dependence on t shown in Fig. 16a.

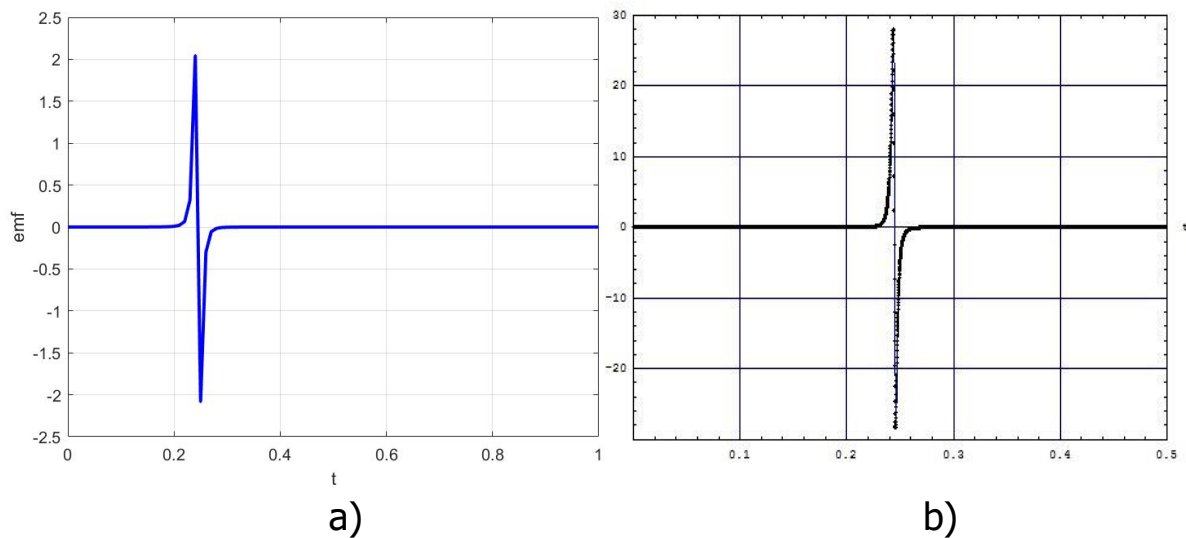


Fig. 16. (a) To a first approximation, there is a similarity with the experimentally measured EMF (see Fig. 14). (b) When the coil gap decreases from 12.5 mm to 3 mm, an emf of 28 V is predicted.

This simulation allows us to make a preliminary calculation of the EMF when the 40-mm-diameter coil is replaced with a 20-mm-diameter coil with the same wire length and the same magnet. The simulation predicts a peak EMF of 28 V (Fig. 16b).

The above result contradicts Faraday's EMF law $\varepsilon = -\frac{d(BS)}{dt}$, where B is the magnetic field through the circuit and S is the loop area. Indeed, we have the same magnet with its B , and the magnet moves at the same speed. With a smaller coil diameter, S , the loop area, decreases. Hence, Faraday's formula predicts a decrease in EMF compared with a larger coil.

In contrast, the simulation predicts that the EMF will increase by a factor of 14.

Let us take a closer look at the situation, with $n = L/2\pi\rho$. Here, L denotes the constant length of the coil wire, ρ is the variable coil radius, and n is the number of coil turns.

The total contour area $S = n\pi\rho^2 = L\rho/2$ is proportional to ρ .

We previously calculated the EMF values for $\rho = 20$ mm and 10 mm by simulation. Having done the same with other values of ρ and applying curve fitting, we obtained the EMF dependence on ρ : $EMF \sim \frac{1}{\rho^4}$, as shown in Fig. 17.

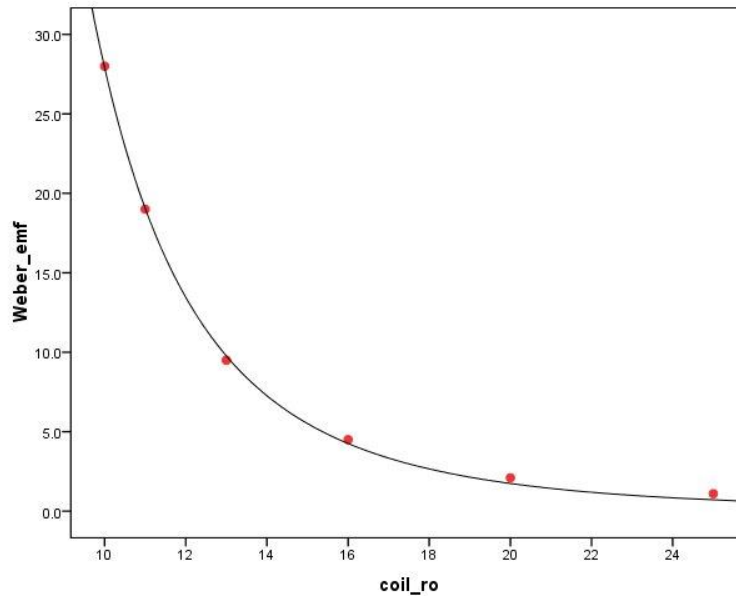


Fig. 17. The EMF dependence on ρ determined by the simulation contradicts the results from Faraday's law of induction.

According to the simulation, the EMF decreases sharply with increasing coil radius ρ (and with an increasing gap between the magnet and coil as well), whereas Faraday's law predicts that the EMF will not decrease at all.

This result is not surprising; the image on the oscilloscope screen (Fig. 14) shows that the EMF arises only for a short duration corresponding to the minimum distance r . At other time points, the EMF is close to zero. In contrast, the proximity of the magnet to the coil turns is not taken into account in Faraday's formula $\varepsilon = -\frac{d(BS)}{dt}$.

7. Discussion.

The question arises: why does the EMF sharply change sign at the moment when the EMF reaches its peak?

Usually, when explaining electromagnetic induction phenomena, Lenz's rule is cited: the induced current opposes changes. But this rule does not answer why the induced current "dislikes changes."

The new paradigm explains this by saying that an electron moves with its negative charge in front. When the electron of a microcurrent passes by the element ds_2 , initially its negative charge faces ds_2 , and repels free electrons in it (see Fig. 18).

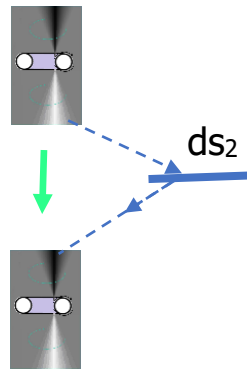


Fig. 18. An electron of the microcurrent passes by the coil element ds_2 . But as it moves away from ds_2 , the electron turns its back (i.e., its positive charge) to ds_2 , and the repulsive force sharply changes to an attractive one precisely at the moment of minimal distance, i.e., maximum EMF.

Thus, the change in the EMF sign always occurs at the peak of the EMF.

This process is expressed in Weber's formula (6). The z-component of the vector \mathbf{r} , connecting two elements ds_1 and ds_2 , equals $r_z = h_0 - gt^2/2$. For the velocity vector, the x and y components are zero $\mathbf{V} = (0, 0, -gt)$. Therefore, the dot product $\mathbf{V} \cdot \mathbf{r} = (-gt)(h_0 - gt^2/2)$.

The first multiplier does not change sign, whereas the sign of the second multiplier is positive initially, but it becomes negative immediately after the distance r to ds_2 becomes minimal and the EMF is maximal.

8. Concept of a magnetic field

In 1926, Bush [12] (p. 130) indicated the problematic nature of the magnetic field: "The total force between moving charges was split into two parts."

This fact is fixed in the Lorentz formula:

$$\vec{F}_L = q\vec{E} + q\vec{v} \times \vec{B} \quad (7)$$

where \vec{B} is the magnetic field.

However, you can choose a reference frame in which the charge q is at rest, and the magnetic force then disappears. Moreover, a problem arises as to whether a magnetic field moves or not (p. 130), which leads to possible paradoxes. One such paradox was published by Mansuripur [13].

Let us assume that a test charge is at rest near a magnetic pole (Fig. 19a). The magnet is neutral; thus, no electric force is exerted on the charge. The charge is in a magnetic field, but $v = 0$; hence, $F_{\text{mag}} = 0$. As a result, no force is exerted on the charge. However, in a reference frame moving to the left, the charge has a non-zero velocity (Fig. 19b); therefore, the charge experiences a non-zero magnetic force, which contradicts our previous conclusion.

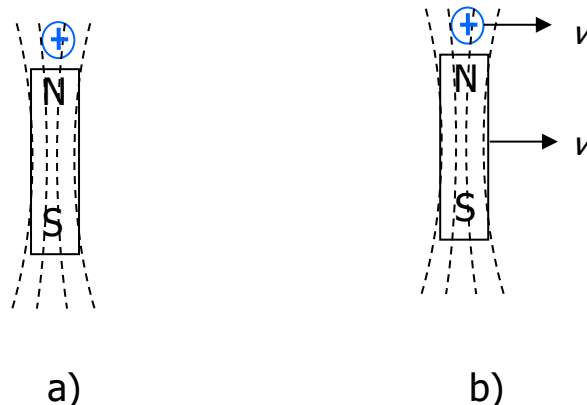


Fig. 19. The absence (a) or presence (b) of a magnetic force depends on the choice of reference frame (Mansuripur's paradox [13]).

Starting in 1905, Kaufmann [14], Bucherer [15], Neumann [16], and others carried out experiments in which electrons traveled between condenser plates.

To calculate the deflection of electrons traveling between plates, experimenters used the formula $F=q E$, which is correct only when charges are stationary (E is the electric field inside the capacitor). Because the electrons are moving, the deflection force should be calculated from the Lorentz formula (Eq. (7)), but the magnetic field is absent.

To eliminate inconsistency, the electron mass was made variable:

$$m = \frac{m_0}{\sqrt{1-\beta^2}} \quad (8)$$

where $\beta = v/c$.

However, based on Weber's formula (Eq. (5)), Bush (p. 148) showed that the integral Weber force acting on an electron moving within a parallel-plate capacitor is perpendicular to the electron velocity and equals the following:

$$F_W = Ee \left(1 + \frac{\beta^2}{2}\right) \quad (9)$$

That is, the electrostatic force must be multiplied by a factor of $\left(1 + \frac{\beta^2}{2}\right)$, with the electron mass being invariant.

Thus, Bush's alternative approach abandons the concept of a magnetic field and obtains agreement with the Kaufmann–Bucherer experiments. Bush showed that Weber's theory, when applied to interpret experiments with fast electrons, "involves an invariant mass" [12].

9. Conclusions

The new paradigm introduces several new aspects to electrodynamics. First, the electric field is a type of gravitational field. Secondly, moving

charges generate a moving gravitational field, which is commonly interpreted as a magnetic field. Thus, the gravitational field of a moving charge replaces both the electric and magnetic fields.

With the new paradigm, unification occurs; instead of three interaction fields, we obtain one expanded field. As a result, the number of postulates in electrodynamics decreases.

Combined with Weber's formula, the new paradigm allows one to calculate the induced EMF resulting from the movement of a magnet and demonstrates the inconsistency of Faraday's law of induction in this experiment.

References

- [1] Y. Bakman, "A New Physical Paradigm," 23 July 2020. [Online]. Available: <https://vixra.org/abs/2008.0038>. [Accessed 23 March 2024].
- [2] Y. Bakman, "Breakthrough in Understanding Gravity," 24 September 2023. [Online]. Available: <https://www.youtube.com/watch?v=fkGKLAOV32U>. [Accessed 29 September 2023].
- [3] N. Tesla, *New York Times*, 21 April 1908.
- [4] Y. Bakman, "Solution to Quantum Gravity and Other Enigmas of the Dominant Paradigm," vixra, 29 September 2021. [Online]. Available: <https://vixra.org/pdf/2109.0210v1.pdf>. [Accessed 18 October 2021].
- [5] Y. Bakman, "How a gravitational field accelerates particles and atoms.," vixra, 9 March 2021. [Online]. Available: <https://vixra.org/abs/2103.0050>. [Accessed 20 May 2021].

- [6] Y. Bakman, "The mechanism of gravitational deflection of light," *vixra*, 10 October 2023. [Online]. Available: <https://vixra.org/abs/2310.0051>. [Accessed 25 October 2023].
- [7] Y. Bakman, "Is the Positron Really an Antiparticle? a Semiclassical Model of the Electron Charge," *viXra*, 13 November 2021. [Online]. Available: <https://vixra.org/abs/2111.0068>. [Accessed 23 October 2022].
- [8] Andre Assis, Wilhelm Weber, *Weber's electrodynamics. Fundamental theories of physics*, v.66, Kluwer Academic Publishers, 1994.
- [9] W. Weber, "Elektrodynamische Massbestimmungen: uber einallgemeines Grundgesetz der elektrischen Wirkung", *Werke*, Bd.3, pp. 25-214. (Determinations of Electrodynamical Measure: on a Fundamental General Law), Berlin: Julius Springer, 1893.
- [10] Y. Bakman, "Interrelations between electrodynamics and gravitation," 2017. [Online]. Available: <https://sites.google.com/site/bakmanyef/recentpublications2>. [Accessed 18 January 2021].
- [11] Feynman, R. P., Leighton, R. B., Sands, M., *The Feynman Lectures on Physics*, τ. Volume II, Addison Wesley, 1963-5.
- [12] V. Bush, "The force between moving charges," *Journal of Mathematics and Physics*, τ. 5, pp. 129-57, 1926.
- [13] M. Mansuripur, "Trouble with the Lorentz law of force: Incompatibility with special relativity and momentum conservation," *Phys. Rev. Lett.*, τ. 108, № 19, p. 193901, 7 May 2012.
- [14] W. Kaufmann, "Uber die Konstitution des Elektrons," *Ann. Physik*, № 19, p. 495, 1906.
- [15] A. Bucherer, "Die experimentelle Bestätigung des Relativitätsprinzips," *Annalen der Physik*, № 28, pp. 513-36, 1909.

[16] G. Neumann, "Die träge Masse schnellbewegter Elektronen,"
Annalen der Physik, № 45, pp. 529-79, 1914.